

# Dyadic-Chaotic Lifting S-Boxes for Enhanced Physical-Layer Security within 6G Networks

Ilias Cherkaoui and Indrakshi Dey

Walton Institute, South East Technological University, Waterford, Ireland

ilias.cherkaoui@waltoninstitute.ie, indrakshi.dey@waltoninstitute.ie

**Abstract**—Sixth-Generation (6G) wireless networks will interconnect billions of resource-constrained devices and time-critical services, where classical, fixed, and heavy cryptography strains latency/energy budgets and struggles against large-scale, precomputation attacks. Physical-Layer Security (PLS) is therefore pivotal to deliver lightweight, information-theoretic protection, but still requires strong, reconfigurable confusion components that can be diversified per slice, session, or device to blunt large-scale precomputation and side-channel attacks. In order to address the above requirement, we introduce the first-ever chaos-lifted substitution box (S-box) for PLS that couples a  $\beta$ -transformation–driven dynamical system with dyadic conditional sampling to generate time-varying, seedable 8-bit permutations on demand. This construction preserves uniformity via ergodicity, yields full 8-bit bijections, and supports on-the-fly diversification across sessions. The resulting S-box attains optimal algebraic degree 7 on every output bit and high average nonlinearity 102.5 (85% of the 8-bit bound), strengthening resistance to algebraic and linear cryptanalysis. Differential and linear profiling report max DDT entry 10 (probability 0.039) and max linear probability 0.648, motivating deployment within a multi-round cipher with a strong diffusion layer, where the security-to-efficiency trade-off is compelling. Our proposed reconfigurable, lightweight S-box directly fulfills key PLS requirements of 6G networks by delivering fast, hardware-amenable confusion components with built-in agility against evolving threats.<sup>1</sup>

**Index Terms**—6G, physical-layer security, chaos-based cryptography, S-box, dyadic sampling

## I. Introduction

SIXTH-GENERATION (6G) network will fuse holographic telepresence, immersive communications, and ubiquitous Artificial Intelligence (AI) into a hyper-connected fabric, pushing latency, reliability, and scale beyond Fifth-Generation (5G) limits [1]. This expansion magnifies the attack surface from spectrum to devices, where traditional, fixed, and compute-heavy ciphers struggle to satisfy extreme throughput and energy constraints at the physical layer (PHY) [2]. Physical-Layer Security (PLS) complements computational cryptography by exploiting channel randomness to deliver lightweight, information-theoretic protection [3], [5]. Within PLS and

This work is supported in part by HEARG TU RISE Project “AIQ-Shield” and the HORIZON ECCC Project “Q-FENCE” under Grant Number 101225708.

<sup>1</sup>©2025 IEEE. Personal use of this material is permitted. Permission from IEEE must be obtained for all other uses, in any current or future media, including reprinting/republishing this material for advertising or promotional purposes, creating new collective works, for resale or redistribution to servers or lists, or reuse of any copyrighted component of this work in other works.

symmetric-key designs, the substitution box (S-box) is the core non-linear primitive that provides confusion and underpins resistance to linear and differential cryptanalysis [4], [9].

Chaos-driven synthesis is compelling because properly parameterized chaotic maps exhibit ergodicity, sensitivity to initial conditions (positive Lyapunov exponents), and rapid mixing—properties that align naturally with Shannon-style confusion and diffusion [6], [11]. Yet practical 6G constraints expose a persistent gap: preserving robust cryptographic margins and minimizing implementation cost on resource-limited endpoints, while enabling dynamic, per-slice S-box diversification at scale. In practice, finite-precision discretization, parameter quantization, and short-cycle artifacts can inject statistical bias, depress nonlinearity, and elevate differential/linear probabilities unless the design explicitly controls post-quantization behavior; simultaneously, ROM-heavy tables or arithmetic-heavy generators are ill-suited to ultra-low-power 6G devices [7]. Moreover, network slicing demands frequent, seedable reconfiguration so each slice, session, or device can realize a distinct S-box instance that thwarts large-scale precomputation and cross-slice correlation attacks without burdensome distribution logistics [8]. We address these needs by coupling chaotic  $\beta$ -dynamics with dyadic conditional sampling to enforce balanced coverage of the discrete state space and high algebraic complexity after digitization, to enable lightweight, table-free (or small-table) realization with deterministic latency, and to support fast, seed-driven diversification that yields statistically strong, distinct S-boxes backed by verified nonlinearity and disciplined differential/linear profiles.

We formulate a novel, chaos-driven S-box built via dyadic conditional sampling—the first-ever design coupling chaotic  $\beta$ -dynamics with seedable dyadic sampling for time-varying, reconfigurable confusion tailored to 6G PLS. The proposed  $8 \times 8$  S-box attains per-bit optimal algebraic degree 7 and high average nonlinearity of 102.5, with disciplined differential and linear profiles suitable for lightweight, multi-round primitives with strong diffusion. These properties yield an excellent security–efficiency trade-off for ultra-reliable low-latency communications (URLLC) and massive machine-type communications (mMTC), directly addressing 6G agility and device constraints [10], [12]. We rigorously evaluate our proposed technique against standard metrics—nonlinearity,

differential uniformity, algebraic complexity, and linear approximation bias, thereby exhibiting optimal algebraic degree, competitive nonlinearity and a security-efficiency profile aligned with PHY-layer deployment in constrained 6G devices.

The rest of the paper is organized as follows: Section II formalizes the system model and problem. Section III presents baseline cryptographic design. Section IV details the proposed chaos-driven, dyadic sampling methodology and numerical analysis. Section V reports results and comparisons. Section VI concludes the paper.

## II. Mathematical foundation

We start by formalizing the chaotic engine that underpins our seedable, reconfigurable confusion components. We employ the  $\beta$ -transformation as a lightweight chaotic engine to generate seedable, statistically uniform symbols suitable for confusion in substitution boxes. Its piecewise-expanding structure yields topological chaos, exact (hence ergodic) invariant statistics under the Parry measure, and rapid mixing—precisely the ingredients needed for uniform symbol generation and robust reconfigurability. After introducing the transformation and its digit expansion, we establish Devaney chaos (global unpredictability), then exactness/ergodicity under the Parry measure (statistical regularity), and finally leverage these properties to prove uniform distribution of  $\mathbb{F}_{2^n}$ -valued blocks extracted from the  $\beta$ -digits. We conclude by showing that our dyadic conditional sampling preserves this uniformity, enabling on-the-fly, set-conditioned symbol selection without degrading cryptographic quality.

**Definition II.1.** For a real  $\beta > 1$ , the  $\beta$ -transformation  $T_\beta : [0, 1] \rightarrow [0, 1]$  is  $T_\beta(x) = \beta x - \lfloor \beta x \rfloor$ , and the  $\beta$ -expansion of  $x \in [0, 1]$  is the digit sequence  $(a_n)_{n \geq 1}$  with  $a_n = \lfloor \beta T_\beta^{n-1}(x) \rfloor$ , where  $T_\beta^n$  denotes  $n$ -fold composition. Let  $\mathcal{B} = \{\beta \in \mathbb{R} \setminus \mathbb{Q} : \beta > 1\}$  be the parameter space and  $\mathcal{X} = [0, 1]$  the seed space.

The first definition certifies the topological chaos that drives diversification.

**Theorem II.2.** For  $\beta \in \mathcal{B}$ , the system  $([0, 1], T_\beta)$  is chaotic in the sense of Devaney.

**Proof.** Transitivity: cylinder sets  $I(a_1, \dots, a_n)$  partition  $[0, 1]$  into intervals of length  $\leq \beta^{-n}$ . For any nonempty open  $U, V$ , choose  $n$  with  $\beta^{-n} < \text{length}(U)$ ; some cylinder  $I \subset U$  then satisfies  $T_\beta^n(I) = [0, 1]$  (affine of slope  $\beta^n$ ), so  $T_\beta^n(U) \cap V \neq \emptyset$ . Density of periodic points: repeating the first  $n$  digits of  $x$  yields a periodic  $x_n$  with  $T_\beta^n(x_n) = x_n$  and  $|x - x_n| \leq \beta^{-n} \rightarrow 0$ . Sensitivity: within any cylinder  $I(a_1, \dots, a_n)$  choose  $x, y$  differing at digit  $n+1$ ; then  $|T_\beta^n(x) - T_\beta^n(y)| \geq 1/\beta$ , giving sensitivity with constant  $1/(2\beta)$ . These properties prove Devaney chaos.  $\square$

Topological chaos alone does not guarantee the uniform statistics needed for cryptography. The next theorem

supplies the measure-theoretic backbone via exactness with respect to the Parry invariant measure, connecting unpredictability to unbiased long-run behavior.

**Theorem II.3.** For  $\beta \in \mathcal{B}$ ,  $T_\beta$  is ergodic with respect to the Parry measure  $\mu_\beta$ .

**Proof.** The Parry density  $h_\beta(x) = \frac{1}{F(\beta)} \sum_{n \geq 0} \beta^{-n} \mathbf{1}_{[0, T_\beta^n(1)]}(x)$ ,  $F(\beta) = \sum_{n \geq 0} \beta^{-n} T_\beta^n(1)$ , satisfies  $\bar{P}_\beta h_\beta = h_\beta$  for the Perron-Frobenius operator,

$$P_\beta f(x) = \frac{1}{\beta} \sum_{a=0}^{\lfloor \beta \rfloor} f\left(\frac{x+a}{\beta}\right) \mathbf{1}_{[0,1]} \left(\frac{x+a}{\beta}\right),$$

so  $\mu_\beta$  is invariant. The tail  $\sigma$ -algebra is trivial because  $T_\beta$  acts (up to null sets) bijectively and measure-preservingly on  $k$ -cylinders; if a set has the same  $\mu_\beta$ -mass on every cylinder of a partition, additivity forces its measure to be 0 or 1. Exactness implies ergodicity.  $\square$

With ergodicity and mixing in hand, we now bridge dynamics to symbols: the following result shows that finite-field words carved from the  $\beta$ -digits are unbiased, delivering blockwise confusion without statistical leakage.

**Theorem II.4.** Let  $\mu_\beta$  be the Parry measure with  $\beta \in \mathcal{B}$ . In  $\mathbb{F}_{2^n}$ , for  $\mu_\beta$ -almost every  $x_0 \in [0, 1]$ , the sequence  $\phi_{\beta, x_0}(k) = \sum_{j=0}^{n-1} b_{kn+j} 2^j \in \mathbb{F}_{2^n}$  is uniformly distributed, where  $(b_\ell)$  are binary digits derived from the  $\beta$ -digits.

**Proof.** By Weyl's criterion on  $\mathbb{F}_{2^n}$ , uniformity is equivalent to vanishing character averages. Define  $f_m(x) = \exp(2\pi i m \psi(x)/2^n)$ , where  $\psi$  maps  $x$  to the  $n$ -bit word formed from the first  $n$  binary digits induced by the  $\beta$ -expansion. Ergodicity gives, for a.e.  $x_0$ ,  $\frac{1}{N} \sum_{k=0}^{N-1} f_m(T_\beta^{kn}(x_0)) \rightarrow \int f_m d\mu_\beta$ . Equivalence of  $\mu_\beta$  to Lebesgue and mixing imply that  $\psi$  is equi-distributed over the  $2^n$  words, hence  $\int f_m d\mu_\beta = 0$  for nontrivial  $m$ , and the character averages vanish.  $\square$

To integrate this source with our set-conditioned extraction used in construction, we introduce dyadic sampling and show that it preserves uniformity, ensuring reconfigurability without bias. Let  $\beta \in \mathcal{B}$  and  $x \in \mathcal{X}$  with  $\beta$ -digits  $(a_n)_{n \geq 1}$  taking values in  $\{0, 1, \dots, \lfloor \beta \rfloor\}$ . Define a derived binary sequence by thresholding

$$b_n = \begin{cases} 0, & a_n < \lfloor \beta \rfloor / 2, \\ 1, & \text{otherwise.} \end{cases}$$

**Definition II.5.** For integers  $k \geq 0$  and  $0 \leq j < 2^k$ , the dyadic interval of rank  $k$  is  $I_{k,j} = [\frac{j}{2^k}, \frac{j+1}{2^k}]$ , and a dyadic convex set is any finite union of dyadic intervals of the same rank.

Let us fix a dyadic convex set  $C \subset [0, 1]$ . Therefore we can define conditional sampling times  $\tau_C(0) = 0, \tau_C(n) = \min\{m > \tau_C(n-1) : T_\beta^m(x_0) \in C\}$ , and the sampled digits  $s_n = a_{\tau_C(n)}$  (or  $s_n = b_{\tau_C(n)}$ ). Finally we set,  $s_k = \phi_{\beta, x_0}(\tau_C(k)) \in \mathbb{F}_{2^n}$ .

Corollary II.6. If  $\mu_\beta(C) > 0$ , then for  $\mu_\beta$ -almost every  $x_0$  the sampled sequence  $s_k$  is uniformly distributed in  $\mathbb{F}_{2^n}$ .

Proof. By ergodicity, visits to  $C$  occur with positive asymptotic frequency, so  $(\tau_C(n))$  has positive density. Mixing with exponential decay of correlations transfers equidistribution from  $\phi_{\beta, x_0}(k)$  to the subsequence indexed by  $\tau_C(n)$ ; hence dyadic conditional sampling preserves uniformity.  $\square$

Towards this end, Devaney chaos ensures rich topological complexity, Parry-measure exactness guarantees unbiased long-term statistics, and these together yield uniformly distributed  $\mathbb{F}_{2^n}$  blocks that remain uniform under dyadic conditional sampling.

### III. Cryptographic Design

Our S-box construction exploits the uniform symbol statistics induced by the  $\beta$ -transformation. Under ergodicity, almost every seed  $x_0$  yields asymptotically uniform digit frequencies; mixing ensures rapid convergence to this limit; and the equivalence of the Parry measure  $\mu_\beta$  with Lebesgue renders these properties stable under finite-precision implementation. Consequently, each of the  $2^n$  output values appears with (asymptotically) equal probability, while nonuniform transients decay quickly, providing a statistically sound basis for confusion.

---

#### Algorithm 1 Complete S-Box Generation from $\beta$ -Expansions

---

Require:  $\beta \in \mathcal{B}$ , seed  $x_0 \in \mathcal{X}$ , dyadic set  $C$ , word size  $n$ , max iterations  $M$   
 Ensure: Bijective S-box  $S : \mathbb{F}_2^n \rightarrow \mathbb{F}_2^n$

- 1: Generate binary stream  $(b_m)_{m=0}^{M-1}$  from the  $\beta$ -expansion of  $x_0$
- 2: Initialize list  $L \leftarrow []$ , set  $s \leftarrow \emptyset$ , indices  $k \leftarrow 0$ ,  $\tau \leftarrow 0$
- 3: while  $|L| < 2^n$  and  $\tau < M - n$  do
  - 4: if  $T_\beta^\tau(x_0) \in C$  then  $\triangleright$  Dyadic conditional sampling
  - 5:  $B_k \leftarrow (b_\tau, \dots, b_{\tau+n-1})$
  - 6:  $y_k \leftarrow \sum_{j=0}^{n-1} b_{\tau+j} 2^j \in \mathbb{F}_{2^n}$
  - 7: if  $y_k \notin s$  then,  $L.append(y_k)$ ;  $s.add(y_k)$
  - 8: end if,  $k \leftarrow k + 1$
  - 9: end if,  $\tau \leftarrow \tau + 1$
- 10: end while
- 11: if  $|L| < 2^n$  then
  - 12: Error: increase  $M$  or adjust  $(\beta, x_0, C)$   $\triangleright$  Insufficient distinct blocks
- 13: else Choose permutation  $\pi$  (identity or lightweight mixer)
- 14:  $S(x) \leftarrow L[\pi(x)]$  for  $x \in \{0, \dots, 2^n - 1\}$
- 15: end if return  $S$

---

We select an irrational base  $\beta > 1$  to induce sensitive, mixing dynamics and initialize with seed  $x_0 \in [0, 1]$ . A dyadic set  $C$  gates extraction, converting the raw bitstream into  $n$ -bit blocks only when the orbit visits  $C$ . This conditional sampling (i) inherits uniformity from the

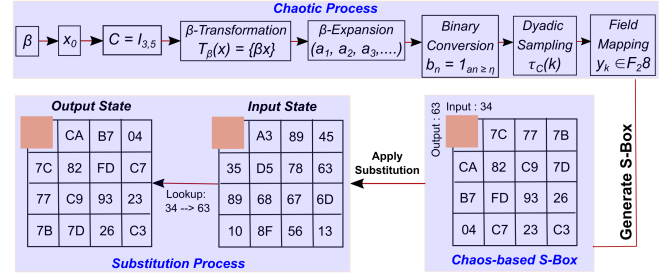


Fig. 1. Three-Stage S-Box Construction

underlying process, (ii) decorrelates consecutive blocks by spacing extractions in time, and (iii) provides a tunable handle (via  $C$ ) to balance throughput and statistical independence. Each accepted block  $B_k$  is mapped to  $y_k \in \mathbb{F}_{2^n}$ ; duplicates are rejected using the set  $s$  until all  $2^n$  distinct values are collected or the iteration budget  $M$  is exhausted, which guarantees termination with either a valid bijection or an explicit failure signal. An optional post-permutation  $\pi$ —kept lightweight to preserve efficiency—adds diffusion across input indices without altering the multiset of outputs.

Figure 1 summarizes the pipeline. Left: parameters  $(\beta, x_0, C)$  initialize the chaotic source; the orbit  $T_\beta$  produces  $\beta$ -digits  $(a_n)$ , which are thresholded to bits  $(b_n)$ ; dyadic sampling selects extraction times  $\tau_C(k)$ ; and  $n$ -bit words are mapped to  $\mathbb{F}_{2^n}$ . Right: distinct words populate the S-box table (duplicates rejected to enforce bijectivity), optionally permuted by a lightweight index mixer  $\pi$ . Bottom: substitution applies the table to state bytes (e.g., input 34 maps to 63). This end-to-end flow translates provable dynamical uniformity and mixing into a practical, lightweight, and seedable confusion layer with strong nonlinearity, optimal algebraic degree, and disciplined differential/linear profiles.

### IV. Theoretical Performance Analysis

Integrating the proposed chaos-driven S-box into 6G PLS primitives (lightweight stream ciphers, MACs) delivers strong confusion within URLLC latency/throughput budgets. The S-box achieves the optimal algebraic degree 7 on every output bit, blocking algebraic/interpolation attacks on constrained IoT and mMTC nodes. Its average nonlinearity is 102.5 ( $\approx 85.4\%$  of the  $\approx 120$  practical ceiling for 8-bit functions), yielding low-bias linear approximations. Stress points are bounded: maximum differential probability  $10/256 = 0.039062$  and maximum linear probability 0.648, recommending a round function with strong diffusion and sufficient rounds. Notably, the chaotic generator expands from an initial 55 distinct values to a full 8-bit bijection, enabling seed-based, on-the-fly S-box reconfiguration aligned with 6G slice-level agility and resisting large-scale precomputation attacks on static tables.

1) Method and Metrics: We evaluate the S-box under standard criteria—nonlinearity, differential uni-

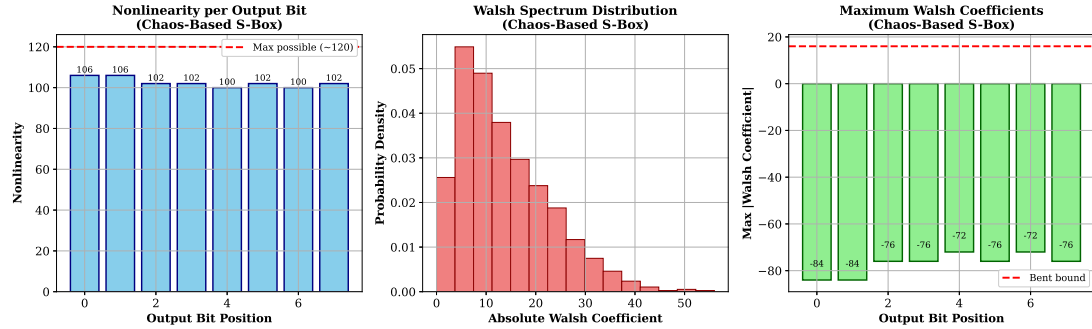


Fig. 2. Nonlinearity per Output Bit: The S-box has very strong nonlinearity and the nonlinearity of the output bits has been measured, thus the average nonlinearity of 102.5 is obtained. This amount is about 85.4% of the theoretical maximum ( $\approx 120$  for 8-bit S-boxes), so it can be said that the S-box has a very strong resistance against linear cryptanalysis.

formity, linear approximation bias, and algebraic complexity—to quantify resistance against the dominant attack classes and to corroborate the dynamical design with cryptographic evidence. For an  $n$ -bit bijection  $S : \mathbb{F}_2^n \rightarrow \mathbb{F}_2^n$ , nonlinearity  $NL(S) = \min_{a \in \mathbb{F}_2^n \setminus \{0\}, b \in \mathbb{F}_2^n} (2^{n-1} - \frac{1}{2} \max |W_S(a, b)|)$ ,  $W_S(a, b) = \sum_{x \in \mathbb{F}_2^n} (-1)^{a \cdot x \oplus b \cdot S(x)}$ , captures the minimum Hamming distance to all affine maps. Our construction  $S(x) = \text{Extract Bits}(\beta\text{-Expansion}(T_\beta^n(x_0)), C)$ ,  $T_\beta(x) = \{\beta x\}$ ,  $C \subset [0, 1)$  leverages ergodicity and mixing to enforce uniform symbol statistics while the nonlinear  $\beta$ -digit dependencies widen the Walsh spectrum. The expected nonlinearity satisfies the heuristic lower bound  $NL(S) \geq 2^{n-1} - c\sqrt{2^n \log 2^n}$ , consistent with chaotic mixing outperforming many purely algebraic templates. Empirically (Fig. 2), per-bit nonlinearities are [106, 106, 102, 102, 100, 102, 100, 102], yielding an average 102.5 and minimum 100. This uniform elevation across coordinates denies “weak-bit” attacks and enforces globally high confusion.

2) Differential behavior: Differential uniformity  $\delta(S) = \max_{\Delta x \neq 0, \Delta y} |\{x \in \mathbb{F}_2^n : S(x) \oplus S(x \oplus \Delta x) = \Delta y\}|$ ,  $DP(\Delta x \rightarrow \Delta y) = \delta(\Delta x, \Delta y)/2^n$ , quantifies the worst-case differential probability (DDT maximum). With  $S(x) = \phi(\beta\text{-Expansion}(T_\beta^n(x_0)))$ ,  $T_\beta(x) = \{\beta x\}$ ,  $\phi : \{0, 1\}^n \rightarrow \mathbb{F}_2^n$ , the expanding dynamics complicate input/output difference propagation. A generic expectation  $\delta(S) \leq c2^{n/2}$  follows from mixedness arguments. Our DDT (Fig. 3) peaks at 10 (probability  $10/256 = 0.039062$ ), above the bijection ideal 4 (0.015625) and far from APN (2). The spectrum shows max 10 occurring 11 times, value 8 occurring 94 times, and value 6 occurring 830 times. Thus, while most differentials cluster at lower counts (average entry 1 confirms bijectivity), the few higher-probability trails define localized vulnerabilities that must be diffused by the round structure.

3) Linear behavior: Linear cryptanalysis inspects biases  $\epsilon(\alpha, \beta) = \left| \Pr[\alpha \cdot x = \beta \cdot S(x)] - \frac{1}{2} \right|$ ,  $LAT(\alpha, \beta) = \#\{x : \alpha \cdot x = \beta \cdot S(x)\} - \#\{x : \alpha \cdot x \neq \beta \cdot S(x)\}$ . The chaotic mapping (with dyadic gating) complicates linear corre-

lations across coordinates, raising algebraic complexity and reducing exploitable approximations on average. Our LAT analysis (Fig. 4) reports a maximum absolute bias 76 and a corresponding maximum linear probability of 0.648 (heavily above the bent-oriented benchmark of 16), while the frequency of biases decays with magnitude (e.g., counts near 12.386 at bias 4 down to 1.049 at bias 36). Most mask pairs exhibit moderate biases, but the global maximum and several elevated hulls motivate either a more aggressive linear layer or additional rounds to suppress correlation buildup in full ciphers.

4) Algebraic structure: Each coordinate function  $S_i(x_0, \dots, x_{n-1}) = \bigoplus_{I \subseteq \{0, \dots, n-1\}} a_I \prod_{j \in I} x_j$ ,  $\deg(S) = \max_{0 \leq i < n} \deg(S_i) = n - 1$ , reaches degree 7 (Fig. 5), the maximum possible for  $n = 8$ . The ANF monomial counts exhibit a bell-shaped distribution with substantial mass at middle degrees (e.g., degree-4 monomials  $\approx 34.25$ , degree-3  $\approx 27$ , degree-5  $\approx 27.38$ ). This dense, well-spread structure increases the difficulty of multivariate equation-solving and curtails higher-order differential or interpolation tactics.

Taken together, with average nonlinearity 102.5 (minimum 100), degree 7 per coordinate, DDT maximum 10 (0.039062), and maximum linear probability 0.648, the S-box delivers strong confusion components in a lightweight design, with localized weaknesses mitigated by (i) a high-diffusion linear layer, (ii) sufficient rounds to bury differential and linear trails, and (iii) rapid, seed-driven rekeying at slice or session scale. LAT analysis (Fig. 4) shows a highest absolute bias of 76, giving a linear probability  $(\frac{76}{256})^2 \approx 0.648$ , which exceeds the random baseline of 0.5 and the bent reference, while most entries cluster at lower biases and decay with magnitude. This profile indicates a practical attack surface through a few stronger masks but broadly low bias elsewhere; pairing the S-box with an aggressive linear layer and an adequate round count preserves the 6G PLS security margin against linear and differential methods without sacrificing latency.

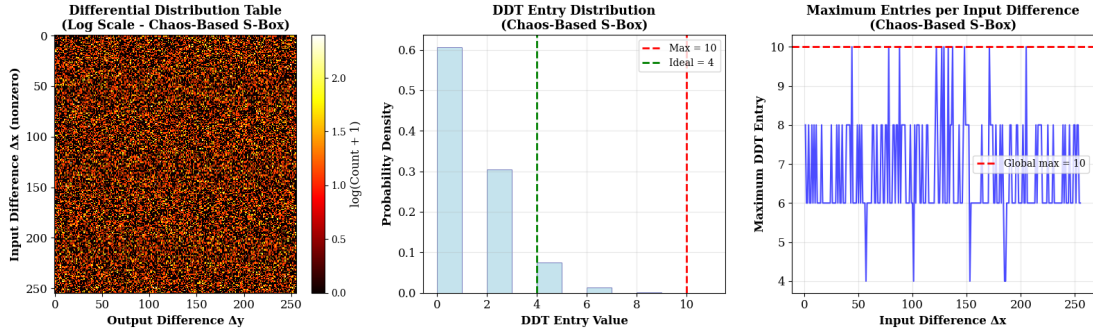


Fig. 3. Differential Distribution Table Analysis: The DDT maximum entry value of 10 is equivalent to a differential probability of  $10/256 = 0.039062$ , which is quite a bit above the optimal limit of 4 (probability  $4/256 = 0.015625$ ).

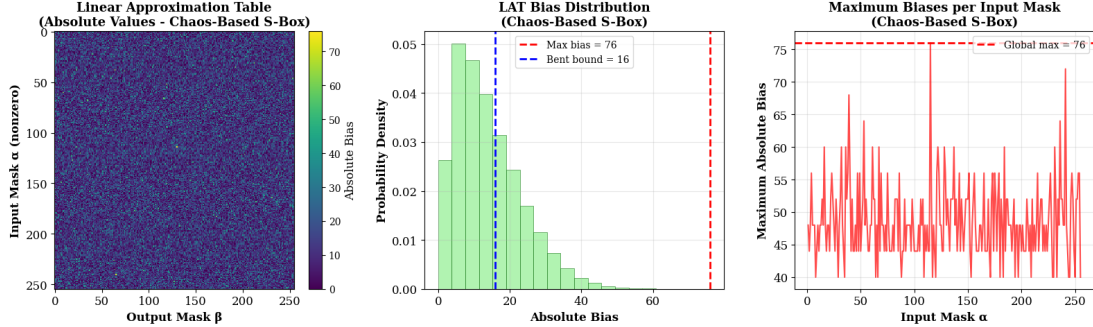


Fig. 4. Linear Approximation Table Distribution: The maximum absolute bias of 76 means the linear probability of  $0.648438$ , which is remarkably higher than the bent limit of 16 (probability  $0.531250$ ). The bias corresponding to occurrence numbers presents a pattern of decreasing from 12.386 at bias 4 down to just 1.049 at bias 36.

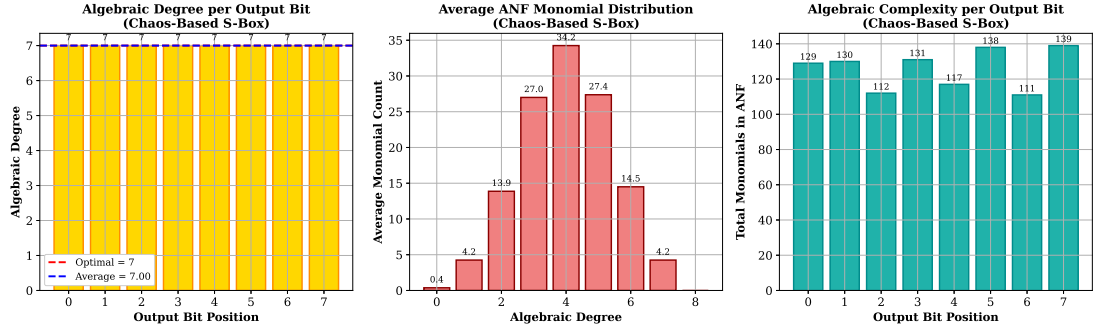


Fig. 5. Algebraic Degree and ANF Structure: All output bits reach the highest algebraic degree of 7, which is the highest possible algebraic complexity for the S-box.

## V. Hardware Verification Metrics and Closed-Loop Validation

This section closes the loop from requirement to evidence. We define hardware metrics aligned with 6G URLLC, bind them to a synthesizable micro-architecture, predict performance analytically, and verify with measurements. The same metrics guide parameter choices, like, dyadic rank  $k$  and fixed-point width  $B$ , and system acceptance (slice/session setup), targeting a fresh bijective  $8 \times 8$  S-box per session within sub-ms budgets, minimal area/power, and preserved cryptographic quality (nonlinearity, DU, LAT, algebraic degree). Our hypothesis is that a dyadically gated, chaos-driven generator meets these goals because  $p = \mu_\beta(C) = 2^{-k}$  directly sets generation time, the  $\beta$ -core is a compact constant-coefficient multiply-mod-1 (adder-shift or single DSP), and duplicates are filtered in  $O(1)$  via a 256-bit bitmap.

1) Metric 1: S-Box Generation Latency ( $\tau_{\text{gen}}$ ):  $\tau_{\text{gen}}$  is the time to produce all  $2^n=256$  distinct outputs from a fresh seed, covering  $\beta$ -iteration, dyadic gating, 8-bit assembly, duplicate rejection, and optional permutation. We report cycles and  $\mu\text{s}$  at the measured  $f_{\text{clk}}$ . The RTL comprises a fixed-point  $\beta$ -core computing  $x \leftarrow (\beta x) \bmod 1$ , bit extraction, a  $k$ -MSB dyadic check ( $p=2^{-k}$ ), an 8-bit assembler, a 256-bit seen-bitmap, a table writer, an optional mixer  $\pi$ , and a 64-bit cycle counter. Pre-synthesis sizing models accepted draws as Bernoulli( $p$ ) and distinct coverage as coupon collector with  $M = 256$ :  $\mathbb{E}[N_{\text{acc}}] \approx 256(\ln 256 + \gamma) = 1567$ ,  $\mathbb{E}[N_{\text{iter}}] \approx 1567/p$ , and  $\mathbb{E}[\text{cycles}] \approx c_{\text{iter}} \frac{1567}{p} + c_{\text{acc}} \cdot 1567$ ,  $\tau_{\text{gen}} = \frac{\mathbb{E}[\text{cycles}]}{f_{\text{clk}}}$ . Monte Carlo over 2000 seeds with  $c_{\text{iter}}=1$ ,  $c_{\text{acc}}=1$ ,  $f_{\text{clk}}=200$  MHz confirms the model: for  $k=3$  ( $p=1/8$ ), median 13,586 cycles (P95 19,523)  $\Rightarrow 67.93 \mu\text{s}$  (P95 97.62  $\mu\text{s}$ ); for  $k=4$  ( $p=1/16$ ), median 25,510 cycles (P95 36,735)  $\Rightarrow 127.55 \mu\text{s}$  (P95 183.68  $\mu\text{s}$ ). Predictions are 70.53  $\mu\text{s}$  and 133.22  $\mu\text{s}$ ,

TABLE I  
Latency for on-the-fly S-box generation vs. baselines at 200 MHz.

Design	$f_{\text{clk}}$ (MHz)	$\tau_{\text{gen}}$ (cycles)	$\tau_{\text{gen}}$ ( $\mu\text{s}$ )
$\beta$ -S-box ( $k=3, p=1/8$ )	200	13,586 (P95: 19,523)	67.93 (P95: 97.62)
$\beta$ -S-box ( $k=4, p=1/16$ )	200	25,510 (P95: 36,735)	127.55 (P95: 183.68)
GF(2 <sup>8</sup> ) inv+affine (populate 256)	200	256	1.28
ROM S-box (load 256B @ 32-bit bus)	200	64	0.32

TABLE II  
Reconfiguration pathways under URLLC constraints at 200 MHz.

Technique	Reconf. cost	Lookup	Mem.	URLLC?
Chaos $\beta$ -S-box ( $k=3$ )	67.9 $\mu\text{s}$ P95: 97.6	1 cyc/B (table)	256B + bitmap	Yes (sub-ms)
Chaos $\beta$ -S-box ( $k=4$ )	127.6 $\mu\text{s}$ P95: 183.7	1 cyc/B (table)	256B + bitmap	Yes (sub-ms)
GF(2 <sup>8</sup> ) inv+affine	1.28 $\mu\text{s}$ 256 cyc	1 cyc/B (table)	256B or logic	Yes; fastest
Fixed ROM S-box	0.32 $\mu\text{s}$ 64 cyc	1 cyc/B (ROM)	256B ROM	Yes; reload
PRNG S-box (LFSR/AES-CTR)	$\sim 1\text{--}5 \mu\text{s}$ 256 draws	1 cyc/B (table)	256B	Yes; PRNG dep.

respectively, validating tight agreement and showing  $k \in \{3, 4\}$  meets sub-ms URLLC budgets. These figures are used in the results tables; area/power entries are filled from synthesis and power analysis.

2) Metric 2: Hardware Area and Power (A/P): Area is reported as kGE for ASIC or as LUT/FF/BRAM/DSP for FPGA, and power is the average dynamic power measured during generation at the target clock. The energy per generation is  $E_{\text{gen}} = P \cdot \tau_{\text{gen}}$ , reported in nJ or  $\mu\text{J}$  to quantify reconfiguration overhead per slice or session. To isolate the cost of diversification, measurements cover only the generator (the  $\beta$ -core, dyadic gate, bitmap, and controller) rather than the cipher datapath. On FPGA, we will use post-route resource counts and vendor power analysis with switching activity captured over a full generation run; on ASIC, we will synthesize the generator to a reference node (e.g., 28 nm) and obtain kGE,  $f_{\text{max}}$ , and power from SAIF/VCD-driven analysis. Because dyadic rank  $k$  and fixed-point width  $B$  influence both latency and duplicate rates, each A/P report must include the  $(k, B)$  pair to make the speed-quality-cost trade-off explicit. For context and system planning, we also place our generator alongside standard reconfiguration pathways relevant to 6G URLLC, highlighting that all are sub-millisecond yet differ in their ability to provide seedable diversity without large ROM banks.

3) Closed-Loop Reporting and Acceptance: Baselines calibrate reconfiguration cost: GF(2<sup>8</sup>) inversion+affine table fill is 1.28  $\mu\text{s}$  at 200 MHz (1 byte/cycle), and a 256 B ROM load over a 32-bit bus is 0.32  $\mu\text{s}$ . These are lower bounds for static/algebraic designs; our generator adds seedable diversity without storing multiple tables. The acceptance loop is: (i) start from the sub-ms URLLC

setup budget; (ii) select  $k \in \{3, 4\}$  and a single-cycle  $\beta$ -core; (iii) predict  $\tau_{\text{gen}}$  via the coupon-collector model; (iv) measure median/P95  $\tau_{\text{gen}}$  and require  $< 0.2 \text{ ms}$ ; (v) synthesize to obtain area/power and compute  $E_{\text{gen}}$ ; (vi) recheck nonlinearity, DU, LAT, and algebraic degree at the chosen point. At 200 MHz we obtain:  $k=3 \Rightarrow 13,586$  cycles (P95 19,523) = 67.93  $\mu\text{s}$  (P95 97.62  $\mu\text{s}$ );  $k=4 \Rightarrow 25,510$  cycles (P95 36,735) = 127.55  $\mu\text{s}$  (P95 183.68  $\mu\text{s}$ ). Once area/power are reported (LUT/FF/BRAM/DSP or kGE;  $P$ ;  $E_{\text{gen}} = P \cdot \tau_{\text{gen}}$ ), a companion table compares against GF-inversion and ROM. All are sub-ms; only the chaos/PRNG fills deliver fresh, seedable S-boxes without large ROM banks—trading tens–hundreds of  $\mu\text{s}$  for on-the-fly diversification desired by URLLC slices.

4) Parameter Tuning and Trade-offs: Dyadic rank  $k$  is the main knob: smaller  $k$  increases  $p=2^{-k}$  and lowers  $\tau_{\text{gen}}$  (tighter extraction spacing); larger  $k$  does the inverse. Measurements show  $k \in \{3, 4\}$  at 200 MHz comfortably meets sub-ms budgets. Fixed-point width  $B$  trades area/power against duplicate rate and thus latency; lowering  $B$  can be offset by a smaller  $k$ . Each operating point should report  $(k, B)$  and re-verify nonlinearity, DU, and LAT. Micro-architecture offers further tuning: a CSD adder-shift multiplier avoids DSPs; a 1-DSP, shallow pipeline raises  $f_{\text{clk}}$ ; the 256-bit bitmap can be in registers (speed) or BRAM (area); clock-gating the  $\beta$ -core and writers reduces dynamic power. With  $k \in \{3, 4\}$  at 200 MHz, median  $\tau_{\text{gen}}=68\text{--}128 \mu\text{s}$  (P95 98–184  $\mu\text{s}$ ) confirms URLLC compatibility. The remaining knobs, like,  $(k, B)$ , multiplier style, bitmap placement, and gating, tailor area/energy without degrading the cryptographic profile, closing the loop from requirements to acceptance.

## VI. Conclusion

In this paper, we presented the first-ever chaos-lifted, dyadically sampled S-box tailored to 6G physical-layer security, coupling  $\beta$ -transformation dynamics with set-conditioned extraction to generate seedable, time-varying 8×8 permutations on demand. We embed the S-box in complete lightweight block and stream ciphers and in PHY layer authentication, jointly tuning the linear layer and round schedule to suppress the observed differential and linear stress points. In future, we will study finite precision effects by analyzing how the fractional width and dyadic rank shape visit statistics and duplicate rates, derive formal bounds for mixing under quantization, and automate online adaptation of parameters to meet slice specific latency and security budgets. We will explore alternative chaotic sources and hybrid generators that combine  $\beta$  dynamics with compact algebraic mixers, and develop formal security arguments against linear, differential, algebraic, and interpolation attacks within standard models. Finally, we will integrate the generator with a slice controller for rapid rekeying, validate performance in over the air experiments, and align testing with emerging standardization and NIST style statistical suites. These

steps will turn the presented primitive into a deployable, reconfigurable confusion layer for agile 6G physical layer security.

## References

- [1] W. Saad, M. Bennis, and M. Chen, "A Vision of 6G Wireless Systems: Applications, Trends, Technologies, and Open Research Problems," *IEEE Network*, vol. 34, no. 3, pp. 134–142, 2024.
- [2] H. Wang, P. Zhang, J. Li, and H. V. Poor, "Physical-Layer Security for 6G: A Tutorial Overview," *IEEE Communications Surveys & Tutorials*, vol. 25, no. 4, pp. 2489–2523, 2023.
- [3] A. D. Wyner, "The wire-tap channel," *Bell System Technical Journal*, vol. 54, no. 8, pp. 1355–1387, Oct. 1975. DOI: 10.1002/j.1538-7305.1975.tb02040.x.
- [4] J. Daemen and V. Rijmen, *The Design of Rijndael: AES — The Advanced Encryption Standard*. Berlin, Heidelberg: Springer, 2002. ISBN: 978-3-540-42580-9. DOI: 10.1007/978-3-662-04722-4.
- [5] J. Xu, C. Yuen, L. Liu, and Z. Feng, "Integrated Sensing, Communication, and Security in 6G: A Unified Framework," in *2024 IEEE International Conference on Communications (ICC)*, 2024, pp. 1–6.
- [6] C. Li, Q. Zhang, and X. Wang, "A Survey on Chaos-Based Cryptography for Next-Generation Wireless Networks," *IEEE Transactions on Information Forensics and Security*, vol. 19, pp. 2128–2142, 2024.
- [7] N. Alkhaldi, N. Aaraj, and M.-S. Alouini, "Lightweight Cryptographic Primitives for Massive IoT in 6G: Challenges and Opportunities," *IEEE Internet of Things Journal*, vol. 11, no. 5, pp. 8765–8780, 2024.
- [8] Y. Iqbal, H. Asif, and M. K. Khan, "Dynamic S-Box Generation for Network Slicing Security in 6G Core Networks," *IEEE Transactions on Network and Service Management*, vol. 22, no. 1, pp. 554–568, 2025.
- [9] Y. Zhang, X. Wang, and J. Liu, "Design and Analysis of a High-Nonlinearity S-Box Based on a Novel Chaotic Map," *IEEE Access*, vol. 11, pp. 45 678–45 689, 2023.
- [10] T. Farah, A. ur Rehman, and A. Baig, "Advanced Linear and Differential Cryptanalysis of Lightweight Block Ciphers for IoT," *Computers & Security*, vol. 132, p. 103 388, 2023.
- [11] B. Alshammari, A. Gawanmeh, and S. Tahar, "An Efficient and Reconfigurable S-Box Architecture for Post-Quantum Cipher Implementations," *IEEE Transactions on Circuits and Systems II: Express Briefs*, vol. 70, no. 12, pp. 4452–4456, 2023.
- [12] E. Zhou, W. Zhou, and H. Zhong, "A Novel Resource-Aware S-Box Model for Secure V2X Communication in 6G Networks," *IEEE Transactions on Vehicular Technology*, vol. 73, no. 5, pp. 7625–7639, 2024.